Multipole interaction of polarized single-domain particles

2004 J. Phys.: Condens. Matter 16 9037

(http://iopscience.iop.org/0953-8984/16/49/019)

INSTITUTE OF PHYSICS PUBLISHING JOURNAL OF PHYSICS: CONDENSED MATTER

J. Phys.: Condens. Matter **16** (2004) 9037–9045 PII: S0953-8984(04)83046-7

Multipole interaction of polarized single-domain particles

N Mikuszeit, E Y Vedmedenko and H P Oepen

Universität Hamburg, Institut für Angewandte Physik, Jungiusstrasse 11a, 20355 Hamburg, Germany

E-mail: Elena.Vedmedenko@physik.uni-hamburg.de

Received 28 June 2004, in final form 6 October 2004
Published 26 November 2004
Online at stacks.iop.org/JPhysCM/16/9037
doi:10.1088/0953-8984/16/49/019

Abstract

The multipole moments and multipole–multipole interactions of uniformly polarized particles have been calculated based on the fundamental theory of electrostatics. As the polarization of the particles is uniform, only surface charges are considered. The polarization may have its origin in magnetization or ferroelectricity or be an intrinsic property of molecules. It is demonstrated that, depending on the geometry of the particles, the higher order interactions can be comparable to or even stronger than the dipole–dipole interaction. The higher order moments give rise to an additional energy contribution in arrays of close packed polarized nanoparticles. The influence of particle aspect ratios as well as array periodicity is discussed.

1. Introduction

Miniaturization plays an important role in modern physics and chemistry as it gives access to new phenomena that can be used in technical applications. It is desirable to increase the density of clusters, dots and micelles, which is correlated with a decrease of their size. Often the particles are polarized or charged. In that case the particles interact. The strength of the interaction increases with decreasing interparticle distance and can be described by means of the multipole expansion. A general calculus for multipole moments can be found in textbooks [1]. However, higher order moments are only calculated to describe molecular orbitals in physical chemistry [2]. In all other cases (magnetic arrays, ferroelectric arrays, colloids etc) the calculations are restricted either to the pure dipole–dipole interaction between the dots [3] or to the first multipole correction to the dipolar coupling [6, 4, 5]. The higher order contributions have not been studied systematically as terms beyond the dipolar one are of minor importance for special cases of zero-thickness in-plane magnetized squares [4] /discs [5]. Only that kind of particles has been addressed in the literature. However, experimentally and industrially produced arrays consist of particles of variable geometry depending on material

and method of preparation. Thus, a general procedure for the calculus of multipole moments of polarized nanoparticles as a function of aspect ratio and symmetry is highly needed as the knowledge of the interaction energy of higher order multipole moments is crucial for further investigations on the magnetic order and magnetic phase transitions in stray field coupled systems.

The multipole expansion may be made either in Cartesian or in spherical coordinates. The advantage of the Cartesian expansion is that only real numbers are required. However, each term of the expansion is a tensor. The order L of the tensor is equivalent to the order of the expansion. The number of independent tensor components of a three-dimensional symmetric tensor increases with the square of L, thus it is a formidable task to treat terms with rank higher than two (quadrupole moments) [4, 6]. The spherical expansion needs complex numbers but its complexity does not change with the order of expansion as the number of independent components is proportional to L. So, it seems that almost any order can be calculated within reasonable effort. However, the treatment of a planar charge distribution in spherical coordinates leads to very complicated integrals. To avoid this difficulty we use the spherical harmonic formalism but express it in Cartesian coordinates. In this way we define a general procedure to calculate the multipole moments and the corresponding interaction energies of axially symmetric particles. This symmetry class has a wide range of application, e.g. in storage media [7–9]. We demonstrate that for prismatic particles with mirror symmetry only multipole moments of the same symmetry are different from zero. All other multipolar contributions are extinct. This permits us to decrease drastically the computational efforts for calculation of magnetostatic interactions in magnetic/electric arrays. For certain geometries the interaction due to higher order moments is of the same order of magnitude as the dipolar coupling. Hence, it must be considered in the description of order phenomena in close packed arrays or hysteresis and switching behaviour of magnetic or ferroelectric particles.

For the sake of simplicity we restrict the discussion to particles with n-fold rotational symmetry that are polarized parallel to the axis of symmetry or have charged base planes. Although we discuss in this paper only axial systems with point-symmetric charge distributions of negative parity the theory can be easily generalized to positive parity or other geometries, e.g. in-plane polarized discs.

2. Multipole moments of symmetric particles

The multipole moments of a charge distribution $\rho(\boldsymbol{r})$ in spherical coordinates $\boldsymbol{r} = (r, \theta, \varphi)$ are defined by [1]

$$Q_{l\,m} = \int_V \mathrm{d}V\, \rho(\boldsymbol{r}) R_{l\,m}(\boldsymbol{r}) \tag{1}$$

where the integration is performed over the volume V that encloses $\rho(\boldsymbol{r})$, weighted by the regular normalized spherical harmonic $R_{l\,m}(\boldsymbol{r})$ [1] (see also (4))

$$R_{l\,m}(\boldsymbol{r}) = \sqrt{\frac{4\pi}{2l+1}} r^l Y_{l\,m}(\theta, \varphi). \tag{2}$$

The spherical harmonics $Y_{l\,m}(\theta, \varphi)$ represent a complete set of orthogonal functions on the sphere [10]. They are numbered by two independent parameters l and m corresponding to the two degrees of freedom on a sphere θ and φ. The far-field potential is [1]

$$\Phi(\boldsymbol{r}) = \frac{1}{4\pi\mu_0} \sum_{l=0}^{\infty} \sum_{m=-l}^{l} I_{l\,m}(\boldsymbol{r}) Q^*_{l\,m} \tag{3}$$

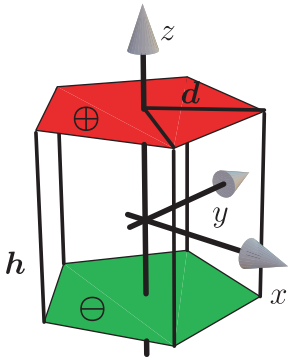

Figure 1. Scheme of a nanoparticle with fivefold (n-fold) symmetry. Every surface can be divided into five (n) equivalent isosceles triangles with edge length d. The particle is polarized in the z-direction.

(This figure is in colour only in the electronic version)

with the irregular normalized spherical harmonics

$$I_{l\,m}(\boldsymbol{r}) = \sqrt{\frac{4\pi}{2l+1}}\frac{Y_{l\,m}(\theta,\varphi)}{r^{l+1}} \tag{4}$$

and $Q^*_{l\,m}$ the complex conjugate of $Q_{l\,m}$. The field can be determined as the negative gradient of the potential $\boldsymbol{F} = -\nabla\Phi$. To ensure the uniqueness of the expansion, the origin of the coordinate system must coincide with the centre of charge

$$\boldsymbol{r}_\mathrm{s} = \frac{\int_V \mathrm{d}V\, \boldsymbol{r}\cdot|\rho(\boldsymbol{r})|}{\int_V \mathrm{d}V\,|\rho(\boldsymbol{r})|}, \tag{5}$$

i.e. $\boldsymbol{r}_\mathrm{s} = 0$; otherwise even the expansion of the potential of a point charge includes higher order moments. The remaining freedom of rotation is handled by tensor transformation rules for spherical harmonics given in [10].

2.1. The relationship between particle symmetry and multipole moments

Let us assume a nanoparticle with n-fold symmetry ($n > 1$) within the x–y-plane, which is polarized in the z-direction (figure 1). The symmetry axis is parallel to the polarization. The upper surface of the particle is positively charged with the surface charge density $\sigma(\boldsymbol{r}) = \mu_0\boldsymbol{n}\cdot\boldsymbol{M}(\boldsymbol{r})$ due to uncompensated dipoles, with the unit vector $\boldsymbol{n}$ perpendicular to the surface and the magnetization vectorfield $\boldsymbol{M}(\boldsymbol{r})$. Hence, with this definition the unit for the magnetic charge is V s and the magnetic dipole moment is measured in V s m. The bottom charge is the mirror image of the positive charge distribution at the top of the particle. To integrate (1) explicitly, we divide the surface into n identical triangles (figure 1). Then the $Q_{l\,m}$ are calculated by the sum over the triangles ($0 \leqslant j \leqslant n-1$) of the top and the bottom surfaces. As the charged surfaces are planar we replace the volume charge density $\rho(\boldsymbol{r})$ and the volume integration (1) by the surface charge density $\sigma(\boldsymbol{r})$ and an integration over the surface element $\mathrm{d}S$.

$$Q_{l\,m} = \sum_{j=0}^{n-1}\left(\int_{j\,\text{th top-triangle}}\mathrm{d}S\,|\sigma(\boldsymbol{r})|R_{l\,m}(\boldsymbol{r}) - \int_{j\,\text{th bottom-triangle}}\mathrm{d}S\,|\sigma(\boldsymbol{r})|R_{l\,m}(\boldsymbol{r})\right). \tag{6}$$

Due to the symmetry of spherical harmonics

$$Y_{l\,m}(\theta,\varphi) = (-1)^{l+m}Y_{l\,m}(\pi-\theta,\varphi) \tag{7}$$

Table 1. The multipole moments $Q_{l\,m}$ (in units of the surface charge density) up to the order $L = 7$ of a particle with fourfold symmetry. All $Q_{l\,m}$ with even l vanish.

l	$m = 0$	$m = 4$[a,b]
1	$2hd^2$	
3[c]	$hd^2\left(\frac{h^2}{2} - d^2\right)$	
5	$\frac{h^5d^2}{8} - \frac{5h^3d^4}{6} + \frac{7hd^6}{12}$	$-\sqrt{\frac{7}{10}}\frac{hd^6}{4}$
7	$\frac{h^7d^2}{32} - \frac{7h^5d^4}{16} + \frac{49h^3d^6}{48} - \frac{3hd^8}{8}$	$\sqrt{\frac{33}{14}}\frac{hd^8}{8} - \sqrt{\frac{77}{6}}\frac{h^3d^6}{16}$

[a] m must be zero or a multiple of 4.
[b] $Q_{l\,-m} = (-1)^m Q^*_{l\,m}$ due to the symmetry of spherical harmonics.
[c] Hence, $Q_{3\,0} = 0$ for $h = \sqrt{2}d$, i.e. a cube.

the sum over the bottom triangles is incorporated into the first sum by the term $(-1)^{l+m+1}$. The azimuthal symmetry $Y_{l\,m}(\theta, \varphi) \propto \exp(\mathrm{i}m\varphi)$ allows us to write

$$\begin{aligned} Q_{l\,m} &= \sum_{j=0}^{n-1} \int_{j\text{th top-triangle}} \mathrm{d}S\,(1 + (-1)^{l+m+1})|\sigma(\boldsymbol{r})|R_{l\,m}(\boldsymbol{r}) \\ Q_{l\,m} &= \int_{\text{one top-triangle}} \mathrm{d}S\,(1 + (-1)^{l+m+1})|\sigma(\boldsymbol{r})|R_{l\,m}(\boldsymbol{r}) \sum_{j=0}^{n-1} \exp\left(\mathrm{i}m\frac{2\pi}{n}j\right) \\ &= \int_{\text{one top-triangle}} \mathrm{d}S\,(1 + (-1)^{l+m+1})|\sigma(\boldsymbol{r})|R_{l\,m}(\boldsymbol{r}) n\delta_{0,\mathrm{mod}(m,n)} \end{aligned} \tag{8}$$

where the Kronecker δ is unity for $n|m$ or $m = 0$ only.

The symmetry properties of (8) lead to several conclusions. Multipole moments with even l exist for $n \geqslant 3$ only and no quadrupole moment ($l = 2$) is allowed. If l is even m must be odd. Except for $m = 0$, the smallest m is $m = n$ as n must be a factor of m because of the Kronecker δ. Therefore, the lowest moment with l even is $(l, m) = (4, 3)$ for a threefold symmetry. The first possible multipole moment with even l for a fivefold symmetry is $(l, m) = (6, 5)$. Additionally, all particles with even rotational symmetry do not possess multipole moments with even l. This can be seen from the parity properties of $Y_{l\,m}(\theta, \varphi)$

$$\hat{P}Y_{l\,m}(\theta, \varphi) := Y_{l\,m}(\pi - \theta, \pi + \varphi) = (-1)^m Y_{l\,m}(\theta, \varphi). \tag{9}$$

If the charge distribution has a negative parity ($\sigma(-\boldsymbol{r}) = -\sigma(\boldsymbol{r})$), which is the case for a particle with n even, the integration reduces to

$$Q_{l\,m} = \int_{\text{one top-triangle}} \mathrm{d}S\,(1 + (-1)^{l+1})|\sigma(\boldsymbol{r})|R_{l\,m}(\boldsymbol{r}) \cdot n \cdot \delta_{0,\mathrm{mod}(m,n)} \tag{10}$$

and l must be odd.

Tables 1 and 2 give the low order moments of a particle with fourfold and cylindrical symmetry, respectively, as a function of the surface area ($\propto d^2$) and the height h of the particle. As expected the dipole moments are proportional to $d^2 \times h$. The dependence of the multipole moments on the effective aspect ratio $h/(\sqrt{2}d)$ of a particle with fourfold symmetry is shown in figure 2. The functions $Q_{l\,m}(h, d)$ may cross zero. This happens for example for the octopole moment of a cube [11] (see figure 2). In the limit of small thicknesses the octopole moment reaches -25% of the dipole moment. This geometry corresponds to sizes of particles often used in experimental studies [12–14]. For vertically elongated particles, such as arrays of magnetic nanocolumns [15, 16] or liquid colloidal crystals with rod-like components [17], the magnitude

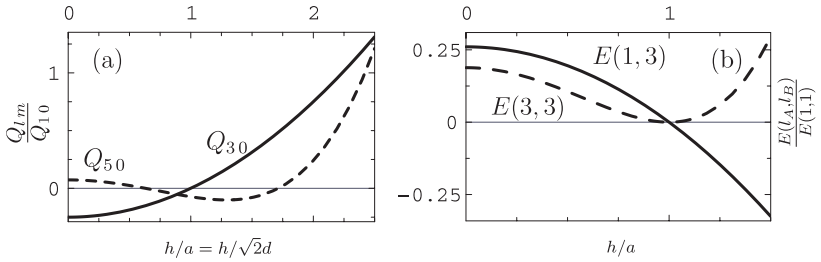

Figure 2. (a) The low order multipole moments $Q_{l\,m}$ (normalized to $Q_{1\,0}$) of particles with fourfold symmetry with height h and edge length a. For $h \to 0$ $Q_{3\,0}$ reaches -25% of $Q_{1\,0}$. (b) The low order multipole–multipole interaction energies $E(l_A, l_B)$ (normalized to the dipole–dipole interaction energy $E(1,\ 1)$) of particles with fourfold symmetry with height h and edge length a. The parameters of $E(l_A, l_B)$ specify the multipole moments l_A and l_B that interact (including the sum over m_A and m_B).

Table 2. The multipole moments $Q_{l\,m}$ (in units of the surface charge density) up to the order $L = 7$ of a particle with cylindric symmetry. All $Q_{l\,m}$ with even l vanish.

l	$m = 0$[a]
1	$\pi h d^2$
3	$\frac{\pi}{4} h d^2 (h^2 - 3d^2)$
5	$\frac{\pi}{16} h d^2 (h^4 - 10h^2 d^2 + 10d^4)$
7	$\frac{\pi}{64} h d^2 (h^6 - 21h^4 d^2 + 70h^2 d^4 - 35d^6)$

[a] m must be zero for symmetry reasons.

of the octopole moment exceeds that of the dipole moment. Thus, many experimental systems require the consideration of higher order multipole moments while in the case of elongated polarized objects the consideration of octopole moments is indispensable.

3. The energy contribution of multipole moments with order $L \geqslant 1$

Exact analytical solutions include implicitly all expansion terms. However, one cannot distinguish between the contributions from different moments, i.e. it is impossible to assign the formation of superstructures in an ensemble of particles to particular features of their geometry. The calculation of the higher order multipole moments of a particle gives the possibility to predict the behaviour induced by multipole terms solely from the knowledge of the single particle and the array geometry. Thus, the use of higher order multipole moments is not meant to substitute analytical solutions, but reveals a new, rather simple treatment to distinguish symmetry effects due to single-particle properties on all length scales. The multipole moments give an additional contribution to the magneto-static interaction. The exact interaction energy, including all multipole terms, can be found in the literature, analytically solved for uniform magnetized bodies with fourfold symmetry [18]. However, the expression for the potential is very complicated and even more complex for the interaction energy.

Though the expansion of the potential of a charge distribution is straightforward, the expansion of the interaction of two charge distributions requires a more complex derivation, particularly in the case of intersecting charge distributions, which are included in the sophisticated treatment of that problem [19]. The formulae given in [19], however, demand a transformation of the coordinate system for each pair interaction. We focus on the most general formulation for non-intersecting charge distributions [2] to obtain results that are independent of the coordinate system.

Table 3. Multipole–multipole interaction energies (in units of $\sigma^2(4\pi\mu_0^{-1})$) of two particles with fourfold symmetry. The particles have an edge length $a = \sqrt{2}d$ and height h. The edges are parallel to the coordinate axes and the distance vector between the particles is $\boldsymbol{R}_{AB} = R \cdot \boldsymbol{e}_x$. Every entry of the table represents an interaction of the moment $Q^A_{l_A}$ with $Q^B_{l_B}$. The index m is omitted as the summation over m is carried out. As the table is symmetric, doubled entries are left blank for clarity.

	Q_1^A	Q_3^A	Q_5^A
Q_1^B	$\frac{4h^2d^4}{R^3}$	$-\frac{3h^2d^4(h^2-2d^2)}{2R^5}$	$\frac{h^2d^4(15h^4-100h^2d^2+28d^4)}{32R^7}$
Q_3^B		$\frac{25d^4(h^3-2hd^2)^2}{16R^7}$	$-\frac{7h^2d^4(105h^6-910h^4d^2+1692h^2d^4-584d^6)}{768R^9}$
Q_5^B			$\frac{7h^2d^4(567h^8-7560h^6d^2+28776h^4d^4-23840h^2d^6+9328d^8)}{4096R^{11}}$

If $\boldsymbol{R}_{AB}$ is the distance vector from charge distribution A with multipole moments Q^A to charge distribution B with multipole moments Q^B the interaction energy is

$$E_{AB} = \frac{1}{4\pi\mu_0} \sum_{l_A l_B m_A m_B} T_{l_A l_B m_A m_B}(\boldsymbol{R}_{AB}) Q^A_{l_A m_A} Q^B_{l_B m_B} \tag{11}$$

with the geometric interaction tensor $T_{l_A l_B m_A m_B}(\boldsymbol{R}_{AB})$ [1]

$$T_{l_A l_B m_A m_B}(\boldsymbol{R}_{AB}) = (-1)^{-l_B} I^*_{l_A+l_B m_A+m_B}(\boldsymbol{R}_{AB}) \times \sqrt{\frac{(l_A+l_B-m_A-m_B)!}{(l_A-m_A)!(l_B-m_B)!}\frac{(l_A+l_B+m_A+m_B)!}{(l_A+m_A)!(l_B+m_B)!}}. \tag{12}$$

The dependence on the distance is given by $I^*_{l_A+l_B m_A+m_B}(\boldsymbol{R}_{AB})$. Hence, it follows from (12) that the energy contribution from the moments $Q^A_{l_A}$ and $Q^B_{l_B}$ of order l_A and l_b respectively decreases with increasing distance as $R_{AB}^{-\lambda}$ and $\lambda = l_A + l_B + 1$. Consequently, higher order multipole moments are important if $R \gtrsim d$. The infinite series converges to the exact solution.

The multipole–multipole interaction energies for two particles with square base of edge length a and height h (edges parallel to the coordinate axes) with distance vector $\boldsymbol{R}_{AB} = R \cdot \boldsymbol{e}_x$ have been calculated and are given in table 3. The multipole–multipole interaction energies as a function of the particle aspect ratio and $R = 1.2a$ are shown in figure 3. An interparticle distance of $R = 1.2a$ is in the range of experimental values (e.g. $R = 1.1a$ in [20] and $R = 1.4a$ in [21]). For small thickness h the dipole–octopole energy is about 26% and the octopole–octopole interaction is close to 19% of the dipole–dipole energy. As the octopole moment vanishes for a cube, the dipole–octopole interaction energy crosses zero at $h/a = 1$, while the octopole–octopole interaction energy has its minimum value, i.e. zero. For vertically elongated particles the multipole–multipole interactions are even stronger. The energy of multipole–multipole interactions between two particles with fourfold symmetry as a function of the interparticle distance R is presented in figure 3. One sees that for $h/a = 0.4$ and $R = 2a$ the pure dipolar approximation gives only 80% of the total energy. Obviously, for $R \leqslant 2a$ the octopole moment must be considered. For $R \leqslant 1.2a$ the 2^5-pole brings further important energy corrections. Hence, our quantitative results can be directly applied to analyse the magnetostatic interactions between square dots of the patterned $Co_{70}Cr_{18}Pt_{12}$ perpendicular media [21].

The interaction energies that correspond to the geometry and material of [21] are calculated in table 4. For $R = 100$ nm the interaction energy between two particles of size of $70 \times 70 \times 20$ nm^3 due to the octopole moments is 17% of the dipole–dipole energy. For

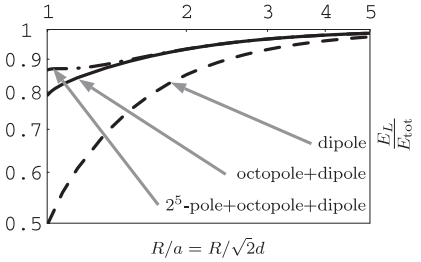

Figure 3. The sums of multipole–multipole energies up to order $L = 1, 3, 5$ normalized to the total energy $E_{\rm tot}$ as function of the interparticle distance R. The aspect ratio is $h/a = 0.4$.

Table 4. The temperature T of the multipole–multipole interaction energies $E = k_{\rm B}T$ of two particles with fourfold symmetry, where $k_{\rm B}$ is the Boltzmann constant. The particles have an edge length $a = 70$ nm and height $h = 20$ nm. The edges are parallel to the coordinate axes and the distance vector between the particles is $\boldsymbol{R}_{AB} = (100\ {\rm nm})\boldsymbol{e}_x$. Every entry in the table represents an interaction of the moment $Q^A_{l_A}$ with $Q^B_{l_B}$. The index m is omitted as the summation over m is carried out. For comparison the energy of $1/2\mu_0 M_S^2 V/k_{\rm B} = 9.44 \times 10^5$ K, where V is the particle volume and $M_S = 4.60 \times 10^5$ A m^{-1}. The numbers in brackets correspond to the values for an infinite square lattice. As the table is symmetric, doubled entries are left blank for clarity.

	Q^A_1	Q^A_3	Q^A_5
Q^B_1	14 719 K (1.33×10^5 K)	2484 K (0.13×10^5 K)	84 K (369 K)
Q^B_3		1165 K (5150 K)	164 K (685 K)
Q^B_5			140 K (572 K)

an infinite square lattice the octopolar energy per particle exceeds 13.5% of the dipolar one. The decrease of the octopolar contribution to the total magnetostatic energy density is due to the faster drop of its strength with the distance. Indeed, the dipolar lattice sum for a square lattice is $S(1, 0, 1; 3/2) = 4\beta(3/2)\zeta(3/2) \approx 9.034$,[1] i.e. in an infinite lattice the field on one lattice site is approximately nine times the field due to one nearest neighbour while for the dipole–octopole interaction the factor is $S(1, 0, 1; 5/2) \approx 5.01$; this equals 56% of the factor for the dipolar interaction. Nevertheless, even a 13.5% effect may significantly change critical properties of an array. For example, a critical temperature $T_{\rm c}$ at which an array becomes ordered due to dipolar plus octopolar interactions will increase by ≈13.5% comparably to a pure dipolar case. Hence, in order to allow for independent particle switching for the perpendicular memory applications one should increase R beyond 100 nm.

In the case of the system from [21] the dipolar interaction alone can induce a long-range order in the array for $R < 150$ nm as the strength of the dipole–dipole coupling $E(1, 1)$ exceeds room temperature (see table 4). A more interesting situation arises for the case of dots with smaller dimensions $30 \times 30 \times 4$ nm^3. In this case the dipole moments of dots decrease and a long-range dipolar ordering cannot be stabilized in an array even for very small interparticle distance of $R = 40$ nm ($E(1, 1) \leqslant 300$ K). The octopole–octopole and dipole–octopole contributions increase the total magnetostatic energy by ≈30% so that the total magnetostatic energy increases to almost 400 K. This is well above the room temperature. Hence, in a certain temperature range a long-range magnetic order in that case can be established. In contrast to the previous situation, however, it is only ensured via higher order magnetostatic contributions.

[1] Where $S(a, b, c; s) = \sum'_{i\,j}(ai^2 + bij + cj^2)^{-s}$ excluding $i = j = 0$ and $\beta(z)$ and $\zeta(z)$ are the Dirichlet beta function and the Riemann zeta function, respectively [22].

Table 5. The same as in table 4, but for particles with an edge length $a = 8$ nm and height $h = 2$ nm. The distance vector between the particles is $\boldsymbol{R}_{AB} = (9\text{ nm})\boldsymbol{e}_x$. In this case the self-energy is $1/2\mu_0 M_S^2 V/k_B = 1233$ K.

	Q_1^A	Q_3^A	Q_5^A
Q_1^B	34.4 K (311.2 K)	9.6 K (48.7 K)	0.7 K (2.9 K)
Q_3^B		7.4 K (32.7 K)	1.9 K (7.8 K)
Q_5^B			2.4 K (9.9 K)

The third interesting situation arises when the particles have dimensions within the superparamagnetic regime, e.g. $8 \times 8 \times 2$ nm^3 for a material with a weak magnetocrystalline anisotropy. Magnetic moments in those dots are strongly coupled by the exchange interaction and can still be described as magnetized objects. In contrast to the previous situation, however, the anisotropy energy per particle is also comparable with the room temperature and the dots are dynamically unstable. The dipolar energy is comparable with the room temperature (see table 5) as in the previous case. The octopole–octopole and dipole–octopole contributions increase the total magnetostatic energy in an infinite square lattice with period of $R = 9$ nm by $\approx$26%. Hence, the multipole–multipole interactions may bring the thermal stability into the system even in the superparamagnetic regime. This result is in accordance with a recent experimental study [23] on close-packed Co, NiFe and CoFe/Cu/NiFe magnetic particle arrays where a stabilization of magnetic configuration against superparamagnetism for small interparticle distances has been found.

Hence, higher order multipolar terms must be considered in systems of two particles as well as infinite lattices if the distance between the particles is of the same order of magnitude as their diameter ($R \gtrsim d$). Calculations of higher order magnetostatic contributions for many experimental situations can be easily made on the basis of table 3.

4. Summary

In conclusion we have developed a procedure to calculate the multipole moments up to any desired order as well as the correlated interaction energies of axially polarized prism-shaped particles including cylinders. The theory is scale invariant, but as we treat single-domain particles, it is of special interest in the nanoscale regime. We demonstrate that prismatic particles with mirror symmetry do not posses multipole moments of even symmetry (quadrupoles etc). Only the moments of odd symmetry (octopole etc) exist. Depending on the geometry and the interparticle distance, the higher order moments can exceed the dipole moment. Therefore, their contribution to the total energy of an array must be included in the case of close packed nanoparticles and the treatment solely by the dipole–dipole approximation is questionable. Higher order contributions may appear as additional anisotropies and cause anisotropy induced orientational order in colloids or liquid crystals. A shift of the superparamagnetic/super(anti)ferromagnetic transition might also be possible due to higher order multipole moments. This will be the subject of future investigations.

References

[1] Stone A J 1996 *The Theory of Intermolecular Forces* (Oxford: Clarendon)
[2] Popelier P L A and Kosov D S 2001 *J. Chem. Phys.* **114** 6539
[3] Bennett A J and Xu J M 2003 *Appl. Phys. Lett.* **82** 2503

[4] Jensen P J and Pastor G M 2003 *New J. Phys.* **5** 68.1
[5] Costa M D and Pogorelov Yu G 2001 *Phys. Status Solidi* a **189** 923
[6] Politi P and Pini G M 2002 *Phys. Rev.* B **66** 214414
[7] Howard J K 1986 *J. Vac. Sci. Technol.* A **4** 1
[8] Scott J F and Paz de Araujo C A 1989 *Science* **246** 1400
[9] Albrecht M, Rettner C T, Best M E and Terris B D 2003 *Appl. Phys. Lett.* **83** 4363
[10] Varsalovich D A, Moskalev A N and Khersonskii V K 1988 *Quantum Theory of Angular Momentum* (Singapore: World Scientific)
[11] Yan Y D and Della Torre E 1989 *IEEE Trans. Magn.* **25** 2919
[12] Jamet J P, Lemerle S, Meyer P, Ferré J, Bartenlian B, Bardou N, Chappert C, Veillet P, Rousseaux F, Decanini D and Launois H 1998 *Phys. Rev.* B **57** 14320
[13] Aign T, Meyer P, Lemerle S, Jamet J P, Ferré J, Mathet V, Chappert C, Gierak J, Vieu C, Rousseaux F, Launois H and Bernas H 1998 *Phys. Rev. Lett.* **81** 5656
[14] Koike K, Matsuyama H, Hirayama Y, Tanahashi K, Kanemura T, Kitakami O and Shimada Y 2001 *Appl. Phys. Lett.* **78** 784
[15] Fruchart O, Klaua M, Barthel J and Kirschner J 1999 *Phys. Rev. Lett.* **83** 2769
[16] Nielsch K, Wehrspohn R B, Barthel J, Kirschner J, Fischer S F, Kronmüller H, Schweinböck T, Weiss D and Gösele U 2002 *J. Magn. Magn. Mater.* **249** 234
[17] van Duijneveldt J S, Gil-Villegas A, Jackson G and Allen M P 2000 *J. Chem. Phys.* **112** 9092
[18] Rhodes P and Rowlands G 1954 *Proc. Leeds Phil. Lit. Soc.* **6** 191
[19] Buehler R J and Hirschfelder J O 1951 *Phys. Rev.* **83** 628
[20] Warin P, Hyndman R, Gierak J, Chapman J N, Ferré J, Jamet J P, Mathet V and Chappert C 2001 *J. Appl. Phys.* **90** 3850
[21] Rettner C T, Anders S, Thomson T, Albrecht M, Ikeda Y, Best M E and Terris B D 2002 *IEEE Trans. Magn.* **38** 1725
[22] Borwein J M and Borwein P B 1987 *Pi & the AGM: A Study in Analytic Number Theory and Computational Complexity* (New York: Wiley)
[23] Cheng J Y, Jung W and Ross C A 2004 *Phys. Rev.* B **70** 64417